

From Limited Labels to Open Domains: An Efficient Learning Paradigm for UAV-view Geo-Localization

Zhongwei Chen, Zhao-Xu Yang*, Hai-Jun Rong, Jiawei Lang
 State Key Laboratory for Strength and Vibration of Mechanical Structures
 School of Aerospace Engineering, Xi'an Jiaotong University

ISChenawei@stu.xjtu.edu.cn, {yangzhx, hjrong}@xjtu.edu.cn, xjtljw@stu.xjtu.edu.cn

Abstract

Traditional UAV-view Geo-Localization (UVGL) supervised paradigms are constrained by the strict reliance on paired data for positive sample selection, which limits their ability to learn cross-view domain-invariant representations from unpaired data. Moreover, it is necessary to reconstruct the pairing relationship with expensive re-labeling costs for scenario-specific training when deploying in a new domain, which fails to meet the practical demands of open-environment applications. To address this issue, we propose a novel cross-domain invariance knowledge transfer network (CDIKTNet), which comprises a cross-domain invariance sub-network and a cross-domain transfer sub-network to realize a closed-loop framework of invariance feature learning and knowledge transfer. The cross-domain invariance sub-network is utilized to construct an essentially shared feature space across domains by learning structural invariance and spatial invariance in cross-view features. Meanwhile, the cross-domain transfer sub-network uses these invariant features as anchors and employs a dual-path contrastive memory learning mechanism to mine latent cross-domain correlation patterns in unpaired data. Extensive experiments demonstrate that our method achieves state-of-the-art performance under fully supervised conditions. More importantly, with merely 2% paired data, our method exhibits performance comparable to existing supervised paradigms and possesses the ability to transfer directly to qualify for applications in the other scenarios completely without any prior pairing relationship.

1. Introduction

The core challenge of cross-view geo-localization [3, 22, 29, 33, 46] lies in bridging the feature gap between heterogeneous viewpoints. With the widespread adoption of unmanned aerial vehicles (UAVs) in complex scenarios such

*Corresponding author.

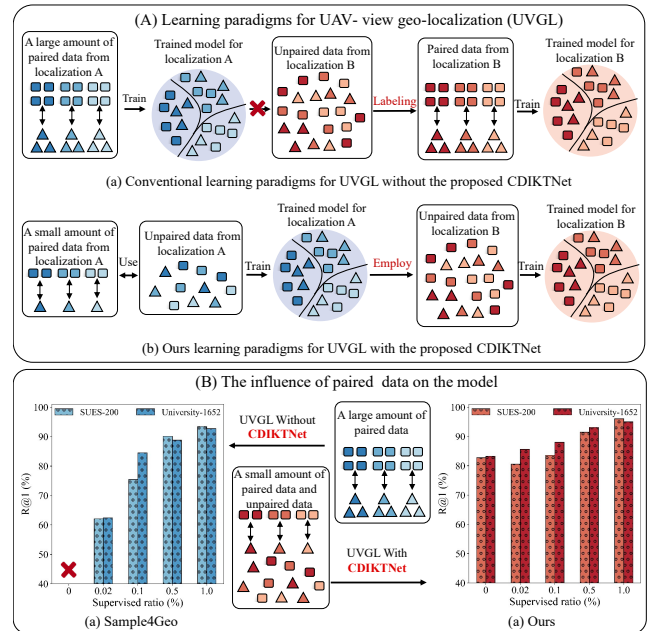


Figure 1. (A) Motivation of the proposed CDIKTNet is to alleviate the dependency on large-scale strictly paired data and enable adaptation to new domains without requiring explicit paired supervision. (B) The performance variations of the representative method Sample4Geo and CDIKTNet under different proportions of paired data are analyzed in the drone→satellite setting across two mainstream benchmarks. Notably, the evaluation on SUES-200 is conducted at an altitude of 150m.

as emergency response [24] and urban surveys [21], the demand for autonomous localization in GPS-denied environments has driven research on UAV-view geo-localization (UVGL). However, the dynamic viewpoints of UAVs introduce scale distortions and non-rigid spatial transformations compared to satellite imagery. This pronounced structural and spatial heterogeneity poses significant challenges for UVGL. In recent years, benefiting from previous research efforts [9, 10, 12, 40], supervised UVGL methods

have made notable progress. Using cross-view contrastive learning, these methods improve the discriminability of the shared feature space, achieving encouraging top-1 accuracy compared to existing methods.

However, as illustrated in Fig. 1 (A(a)) and (B(a)), existing methods [7, 13, 31, 41] strictly rely on large-scale paired image correspondences to learn cross-view feature relationships. In the absence of such pairing constraints, they struggle to effectively capture cross-view features from unpaired images. When paired data become scarce or correspondence is lost, their feature learning ability is severely affected, leading to drastic performance drop or even complete failure. Moreover, environmental variations induce domain shifts, often necessitating repaired efforts to establish such pairwise relationships before deploying methods in new regions. This strong dependency not only restricts the generalization ability of the methods, but also impedes its applicability in resource-constrained annotation scenarios and cross-domain adaptation tasks.

In this paper, we propose a novel cross-domain invariant knowledge transfer network (CDIKTNet) for the UVGL task. The CDIKTNet comprises two core components, including the cross-domain invariance sub-network (CDIS) and the cross-domain transfer sub-network (CDTS). The CDIS is designed to capture structural and spatial invariance across different viewpoints by leveraging the structural invariance feature learning block (SIFL) and the spatial invariance enhancement learning module (SIEL). The CDIS mitigates scale distortions and spatial transformations while generating invariant knowledge representations that are shared between viewpoints. Building upon this foundation, the CDTS utilizes the learned invariant representation as an anchor to construct a feature base space. To further enhance knowledge learning, we introduce a dual-path contrastive memory learning strategy in CDTS, which explores latent cross-view correlations and invariant feature representation among unpaired data. As illustrated in Fig. 1 (A(b)) and (B(b)), CDIKTNet significantly reduces the dependency on strictly paired large-scale data. More importantly, it can be seamlessly transferred to other datasets, including entirely unseen scenarios, without requiring any prior pairing information in the target domain. In summary, the main contributions are outlined as follows.

- We propose a cross-domain invariant knowledge transfer network, which leverages few-shot guided cross-view invariant learning, simultaneously exploring latent correlations and invariant feature representation within unpaired data. It significantly reduces the dependency on strictly paired annotations and enables seamless transfer to new scenarios without any prior pairing information.
- The cross-domain invariance sub-network is designed to learn the representational correlations of structural and spatial features to capture and share the discriminative

viewpoint-invariant features. It is used to construct a feature representation space with high generalization and provides a robust initialization process for subsequent self-supervised learning.

- The cross-domain transfer sub-network is presented to utilize the shared invariant representation as an anchor, in which the pseudo-labels with high-quality are generated by the clustering. Then a dual-path contrastive memory learning strategy is employed to further explore the latent mappings of cross-view features using unpaired data.
- Extensive experiments demonstrate that the proposed CDIKTNet outperforms existing methods in fully supervised settings on two mainstream benchmarks. Moreover, it achieves comparable or even superior performance using a small amount of paired data, while effectively leveraging unpaired data in its own domain. Additionally, it maintains strong unsupervised learning performance when transferred to new scenarios with unpaired data.

2. Related Work

2.1. Cross-view Geo-localization

Cross-view geo-localization (CVGL) is commonly regarded as an image retrieval problem based on heterogeneous visual data. However, geometric-semantic heterogeneity and feature distribution shift across different viewpoints pose significant challenges to CVGL. In traditional ground-to-satellite CVGL [19, 20, 23, 34], many researchers have employed explicit geometric alignment methods [1, 32, 46] to enforce structural consistency across views, while others [30, 36] have used GANs [17] to map source domain images to the target domain. Moreover, PCL [35] attempted to align aerial and satellite images using perspective projection transformation and also employed GAN to synthesize satellite-style images, in order to reduce spatial discrepancies and enhance the representation of geometric structures. But it was difficult to handle non-rigid deformations caused by dynamic UAV viewpoints and remained constrained by the synthetic-to-real domain gap. Recently, researchers [16, 26] have started to model latent geometric structures or spatial consistency to enhance the robustness of UVGL. However, these methods often focused solely on optimizing geometric structure or spatial representation, neglecting their synergistic relationship, resulting in limited generalization under scale variations and spatial shifts in UVGL task. Furthermore, these methods still relied heavily on large amounts of paired data for training, which restricted their applicability in open environments.

2.2. Self-Supervised Cross-Domain Retrieval

In recent years, cross-domain image retrieval based on the supervised paradigm has achieved significant progress [2, 8, 15, 42, 47]. However, reliance on large-scale anno-

tated data limited its applicability, which has prompted researchers to explore self-supervised cross-domain retrieval methods [4, 5, 18]. Current methods [6, 11, 43] have used powerful feature backbone networks for feature initialization, with clustering algorithms [14, 27] to generate pseudo-labels and feature queues to provide stable negative samples for optimizing feature learning. They have improved the quality of pseudo-labels, however, in which feature extractors were heavily dependent, resulting in greater challenges in UVGL. Due to the inherent complexity of cross-view variations, extracting discriminative features at the initialization stage is difficult, posing risks of the low-quality pseudo-labels and potential negative optimization. Furthermore, to address the limitations of traditional methods in handling heterogeneous data, some researchers [44, 45] have proposed cross-modal person retrieval methods based on dual-path contrastive memory learning. Nevertheless, these methods still rely on pre-trained person retrieval models for feature extraction during initialization, constraining their generalization ability.

To address the aforementioned challenges, it is expected that self-supervised training is initialized with a minimal amount of supervised data. However, this method also encounters difficulties in effectively learning invariance within cross-view features because of the scarcity of paired data. Inspired by the supervised learning paradigm discussed in Section 2.1, we adopt a structural and spatial learning perspective to acquire robust and generalized cross-view features, which provides a more stable optimization anchor for self-supervised training and improves generalization.

3. Proposed Method

Problem Formulation: Given a drone-view image set $\mathcal{X}^d = \{x_i^d\}_{i=1}^N$ and a satellite-view image set $\mathcal{X}^s = \{x_j^s\}_{j=1}^M$, where each drone image x_i^d is paired with a corresponding satellite image x_j^s as a positive pair (x_i^d, x_j^s) , the goal is to learn a shared embedding space \mathcal{V} that minimizes the distance between positive pairs while maximizing the distance between negative pairs. In this process, existing methods rely heavily on a large amount of paired data as positive samples for training to achieve high performance. In contrast, our approach differs fundamentally, as we mitigate this dependency. The following sections provide a detailed explanation of our method.

3.1. Cross-Domain Invariance Sub-network

The fundamental theoretical basis of our CDIS lies in the complementarity between structural and spatial features. Given the significant variations in viewpoints and spatial scales in UVGL, the structural features capture domain-invariant topological structures and geometric invariances, while the spatial features establish scale-aware geometric constraints to ensure cross-domain transferability. These

two types of features form a dynamically complementary joint representation space—structural features provide stable semantic invariance, whereas spatial features preserve precise geometric correspondences. This synergy effectively bridges feature distribution discrepancies across different viewpoints, constructing a cross-domain invariance kernel with strong generalization capability.

3.1.1. Structural Invariant Feature Learning

Given a pair of cross-view images $\{x_i^d, x_j^s\}$, high-dimensional feature representations are first extracted using the ConvNeXt-Base [25] backbone network from different perspectives. The extracted features are denoted as $\mathbf{f}_v^u \in \mathbb{R}^{C \times H \times W}$, where $u \in \{d, s\}$ and v is defined such that when $u = d$, $v = i$ and when $u = s$, $v = j$. To effectively leverage structural features across views, the spatial dimensions $H \times W$ are flattened to a single dimension L_i , producing the reshaped representation of features $\mathbf{f}_v^{ul} \in \mathbb{R}^{C \times L}$, which serves as the input to the structural invariance sub-network.

Subsequently, a depthwise separable 3×3 convolution φ_q^3 is used to capture local structural priors, while residual connections preserve the original topological information. After normalization $\mathcal{N}(\cdot)$, the local geometric structures are explicitly modeled, which yields the feature representation \mathbf{f}_{v+}^u . To further enhance the capability of structural invariance learning, we proposed a channel-wise feature refinement module (CRF). Specifically, we project \mathbf{f}_{v+}^u into the latent space through two cascaded linear transformation layers $\mathcal{I}(\cdot)$, thereby capturing high-order interactions between channels. A subsequent 1×1 convolution ψ_q^1 is applied to explicitly capture local structural features. Following this, a gating mechanism $\mathcal{G}(\cdot)$ is utilized to compute the channel attention weights, allowing the network to adaptively focus on view-invariant structural features. Finally, the residual network and normalization $\mathcal{N}(\cdot)$ are employed to fuse cross-layer information, enhancing representational capacity and effectively preserving crucial information. This process can be formulated as

$$\mathbf{f}_{v+}^u = \mathcal{N}(\varphi_q^3(\mathbf{f}_v^{ul}) + \mathbf{f}_v^{ul}) \quad (1)$$

$$\mathbf{f}_{v++}^u = \mathcal{N}(\mathcal{G}(\psi_q^1(\mathcal{I}(\mathbf{f}_{v+}^u)))) + \varphi_q^3(\mathbf{f}_v^{ul}) + \mathbf{f}_v^{ul} \quad (2)$$

To further enhance local geometric invariance, we adopt the same feature processing procedure as in Eq. 1 to extract the feature \mathbf{f}_{v+++}^u . It is important to note that although \mathbf{f}_{v+++}^u contains rich local geometric information, it still lacks global structural features. To address this, we replace the CFR module described previously with an MLP $\mathcal{P}(\cdot)$ combined with the SE attention mechanism. In this module, the global average pooling $\mathcal{A}(\cdot)$ is first applied within the SE mechanism to extract the global information at the channel level. The channel information is then compressed through two linear transformation layers $\mathcal{I}^+(\cdot)$, followed by

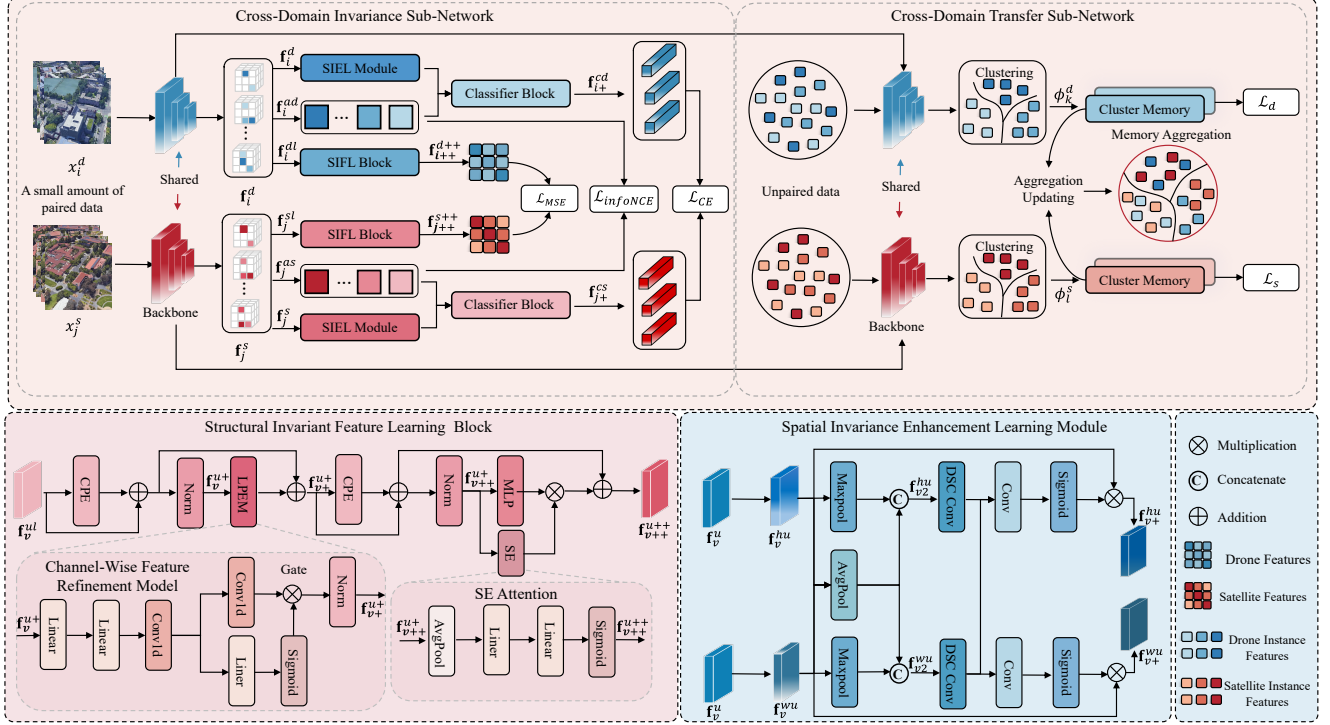


Figure 2. The proposed network pipeline consists of two sub-networks. The cross-domain invariance sub-network is designed to learn feature representations with geometric structural invariance and spatial invariance. The cross-domain transfer sub-network leverages the invariant knowledge learned by cross-domain invariance sub-network as a feature representation embedding space to further explore the latent relationship of cross-view features from unpaired data.

the channel attention weights calculated using the Sigmoid function \mathcal{F} , which are then combined with the global information obtained through the MLP. This further enhances the expression of global channel-level information. Finally, a residual connection is used to fuse the rich local geometric information from the original features with the enhanced global features, thereby achieving the effective integration of local geometry and global structural information. This process can be formulated as

$$\mathbf{f}_{v+}^{u++} = \mathcal{N}(\varphi_q^3(\mathbf{f}_{v+}^{u+}) + \mathbf{f}_{v+}^{u+}) \quad (3)$$

$$\mathbf{f}_{v_{++}}^{u++} = \mathcal{F}(\mathcal{I}(\mathcal{A}(\mathbf{f}_{v_{++}}^{u+}))) \times \mathcal{P}(\mathbf{f}_{v_{++}}^{u++}) + \varphi_k^3(\mathbf{f}_{v_{++}}^{u+}) + \mathbf{f}_{v_{++}}^{u+} \quad (4)$$

This design enhances structural invariance learning by optimizing channel-level feature representation, enabling the effective capture of global structural information while preserving local geometric features, thereby improving generalization and robustness across different perspectives.

3.1.2. Spatial Invariant Feature Learning

Spatial information is particularly crucial for cross-view tasks. To enhance spatial invariance in relation to input features, inspired by [31], we design a dual-path spatial invariance enhancement learning module to capture spatial information across different dimensions.

In the spatial invariance enhancement learning module, we preserve the spatial dimensions H and W of the input features, as opposed to flattening the spatial dimensions to retain channel information. By permuting the input features $\mathbf{f}_v^u \in \mathbb{R}^{C \times H \times W}$ along the channel-height (C-H) and channel-width (C-W) dimensions, we obtain $\mathbf{f}_{v_2}^{hu} \in \mathbb{R}^{H \times C \times W}$ and $\mathbf{f}_{v_2}^{wu} \in \mathbb{R}^{W \times H \times C}$, respectively. This allows the module to capture multi-perspective dependencies across different dimensions. Subsequently, global feature representations $\mathbf{f}_{v_2}^{hu} \in \mathbb{R}^{2 \times H \times W}$ and $\mathbf{f}_{v_2}^{wu} \in \mathbb{R}^{2 \times H \times W}$ are generated by concatenating the results of max pooling and average pooling applied to the permuted features. A 3×3 depthwise separable convolution φ_v^3 is then employed to obtain a more compact feature representation. Subsequently, a strong cross-interaction between height (H) and width (W) is performed, followed by separate 1×1 convolution ψ_k^1 to further enhance the spatial invariance of the feature representation. Finally, the fused features are normalized using a sigmoid function \mathcal{F} to generate attention weights, which are multiplied with the original feature maps and restored to the original dimensions $\mathbb{R}^{C \times H \times W}$, yielding the spatially enhanced feature representation $\mathbf{f}_{v+}^{hu} \in \mathbb{R}^{C \times H \times W}$ and $\mathbf{f}_{v+}^{wu} \in \mathbb{R}^{C \times H \times W}$ as

$$\mathbf{f}_{v+}^{hu} = \mathcal{F}(\psi_k^1(\varphi_v^3(\mathbf{f}_{v_2}^{hu}))) + \psi_k^1(\mathbf{f}_{v_2}^{wu}) \times \mathbf{f}_v^u \quad (5)$$

$$\mathbf{f}_{v+}^{wu} = \mathcal{F}(\psi_k^1(\varphi_v^3(\mathbf{f}_{v2}^{wu})) + \psi_k^1(\mathbf{f}_{v2}^{hu})) \times \mathbf{f}_v^u \quad (6)$$

By capturing dependencies across multiple dimensions, this module effectively enhances robustness to spatial transformations such as rotation and scaling. Moreover, the integration of depthwise separable convolutions and attention mechanisms enables efficient adaptive feature refinement, enhancing feature discriminability.

3.1.3. Multi-level Optimization

In the CDIS, the features \mathbf{f}_{v+}^{u++} obtained from the SIFL are optimized using the mean squared error loss \mathcal{L}_{MSE} [41], which enhances the stability and consistency of the learned features. Furthermore, to enhance structural representation in the spatial invariance enhancement learning module, the features \mathbf{f}_v^{au} extracted by the backbone and processed via global average pooling are combined with \mathbf{f}_{v+}^{hu} and \mathbf{f}_{v+}^{wu} to form the combined features \mathbf{f}_{v+}^{cu} , which are then passed through a classifier module [31]. These features are optimized with cross-entropy loss \mathcal{L}_{CE} to enhance feature discrimination and improve class separability. In addition, to further enhance the feature representations, \mathbf{f}_v^{au} undergo independent optimization using the InfoNCE loss [28] $\mathcal{L}_{InfoNCE}$. The InfoNCE loss promotes clustering of positive samples while separating negatives. The final objective is to minimize the weighted sum of all three losses, ensuring the learning of cross-domain invariant features with strong discriminability and generalization, which can be formulated as

$$\mathcal{L}_{cd} = \lambda_1 \mathcal{L}_{MSE} + \lambda_2 \mathcal{L}_{CE} + \lambda_3 \mathcal{L}_{infoNCE} \quad (7)$$

where λ_1 , λ_2 and λ_3 are the coefficients to control the relative importance of the loss terms.

3.2. Cross-Domain Transfer Sub-network

Our cross-domain invariance sub-network leverages a well-established feature embedding space to maximize the learning potential of the majority of unpaired cross-view data. To further enhance cross-domain adaptation, we propose a novel cross-domain transfer sub-network, which incorporates a dual-path contrastive memory learning strategy specifically designed for UVGL.

Cross-View Feature Memory Initialization. At the beginning of each training epoch, we initialize cross-view feature instances using the invariant knowledge representations learned by the CDIS and perform clustering to generate pseudo-labels. This process aims to mitigate the issue of low-quality pseudo-label initialization caused by suboptimal feature extraction. Subsequently, we construct cluster memories for each view, specifically for drone and satellite perspectives denoted as ϕ_k^d and ϕ_l^s , by computing the average feature representations of drone and satellite instances

within each cluster. This process can be formulated as

$$\phi_k^d = \frac{1}{|\mathcal{H}_k^d|} \sum_{\mathbf{f}_i^d \in \mathcal{H}_k^d} \mathbf{f}_i^d, \phi_l^s = \frac{1}{|\mathcal{H}_l^s|} \sum_{\mathbf{f}_j^s \in \mathcal{H}_l^s} \mathbf{f}_j^s \quad (8)$$

where \mathbf{f}_i^d and \mathbf{f}_j^s are drone and satellite instance features, respectively. $i = 1, \dots, N$, $j = 1, \dots, M$. $\mathcal{H}_{k(l)}^{d(s)}$ denotes the k -th cluster set in drone or satellite view, $|\cdot|$ indicates the number of instances per cluster.

Cross-View Feature Memory Updating. During each training iteration, the cluster memories using a momentum updating strategy are represented as

$$\phi_k^{d(\omega)} \leftarrow \alpha \phi_k^{d(\omega-1)} + (1 - \alpha) q_d \quad (9)$$

$$\phi_k^{s(\omega)} \leftarrow \alpha \phi_k^{s(\omega-1)} + (1 - \alpha) q_s \quad (10)$$

where α is momentum updating factor and ω is iteration number.

Cross-View Contrastive Loss. Given the drone and satellite query q_d and q_s , we compute the contrastive loss for the drone view and the satellite view as

$$\mathcal{L}_{cv}^d = -\log \frac{\exp(q_d \cdot \phi_+^d / \tau)}{\sum_{k=0}^K \exp(q_d \cdot \phi_k^d / \tau)} \quad (11)$$

$$\mathcal{L}_{cv}^s = -\log \frac{\exp(q_s \cdot \phi_+^s / \tau)}{\sum_{k=0}^K \exp(q_s \cdot \phi_k^s / \tau)} \quad (12)$$

where τ denotes the temperature hyper-parameter. Cluster memory $\phi_{k(l)}^{d(s)}$ are utilized as feature vectors at the cluster level to compute the distances between the query instance $q_{d(s)}$ and all clusters. Here, $\phi_+^{d(s)}$ corresponds to the positive cluster memory associated with $q_{d(s)}$.

The cross-domain transfer sub-network is jointly optimized with \mathcal{L}_{cv}^d and \mathcal{L}_{cv}^s . Thus, the final optimization for CDIKTNet is denoted as $\mathcal{L}_{total} = \mathcal{L}_{cd} + \mathcal{L}_{cv}$.

4. Experimental Results

4.1. Datasets and Evaluation Protocol

Datasets. We evaluate CDIKTNet on two challenging benchmarks for UVGL. University-1652 [49] consists of drone, satellite, and ground-level images from 1,652 locations in 72 universities. The training set includes 701 buildings from 33 universities, while the test set comprises 951 buildings from 39 universities. SUES-200 [50] contains 200 locations with altitude variations in aerial images. The training and test sets contain 120 and 80 locations, respectively. Each location gives a satellite image and aerial images at four altitudes, covering diverse environments such as parks, lakes and buildings.

Evaluation Protocols. We employ Recall@K (R@K) and Average Precision (AP) as evaluation metrics. R@K measures the proportion of correct matches within the Top-K

SUES-200																	
Model	GT Ratio	Drone → Satellite								Satellite → Drone							
		150m		200m		250m		300m		150m		200m		300m		300m	
		R@1	AP	R@1	AP	R@1	AP	R@1	AP	R@1	AP	R@1	AP	R@1	AP	R@1	AP
Vit-Baseline[50]	100(%)	55.65	61.92	66.78	71.55	72.00	76.43	74.05	78.26	75.00	55.46	85.00	66.05	86.25	69.94	88.75	74.46
LPN[38]	100(%)	61.58	67.23	70.85	75.96	80.38	83.80	81.47	84.53	83.75	66.78	88.75	75.01	92.50	81.34	92.50	85.72
IFSs [16]	100(%)	77.57	81.30	89.50	91.40	92.58	94.21	97.40	97.92	93.75	79.49	97.50	90.52	97.50	96.03	100.00	97.66
MCCG[31]	100(%)	82.22	85.47	89.38	91.41	93.82	95.04	95.07	96.20	93.75	89.72	93.75	92.21	96.25	96.14	98.75	96.64
Sample4Geo[12]	100(%)	92.60	94.00	97.38	97.81	98.28	98.64	99.18	99.36	97.50	93.63	98.75	96.70	98.75	98.28	98.75	98.05
DAC[41]	100(%)	96.80	97.54	97.48	97.97	98.20	98.62	97.58	98.14	97.50	94.06	98.75	96.66	98.75	98.09	98.75	97.87
CAMP[40]	100(%)	95.40	96.38	97.63	98.16	98.05	98.45	99.33	99.46	96.25	93.69	97.50	96.76	98.75	98.10	100.00	98.85
CDIKTNet	100(%)	96.03	96.87	97.80	98.27	98.90	99.15	99.73	99.79	97.50	94.23	98.75	96.58	100.0	98.33	98.75	98.84
CDIKTNet	10(%)	83.60	86.24	90.53	92.14	94.33	95.32	97.13	97.60	91.25	83.24	95.00	89.53	97.50	93.59	97.50	95.80
CDIKTNet	2(%)	80.55	83.58	88.05	90.10	91.28	93.13	94.48	96.12	90.00	77.16	91.25	85.92	97.50	91.36	97.50	94.07
CDIKTNet	0(%)	82.75	85.25	89.35	91.13	93.15	94.39	95.18	96.12	88.75	80.33	93.75	88.17	95.00	92.15	98.75	94.37

Table 1. Comparisons between the proposed CDIKTNet and some state-of-the-art methods on the SUES-200 datasets.

University-1652					
Model	GT Ratio	Drone → Satellite		Satellite → Drone	
		R@1	AP	R@1	AP
MuSe-Net[39]	100(%)	74.48	77.83	88.02	75.10
LPN[38]	100(%)	75.93	79.14	86.45	74.49
TransFG[48]	100(%)	84.01	86.31	90.16	84.61
IFSs[16]	100(%)	86.06	88.08	91.44	85.73
MCCG[31]	100(%)	89.40	91.07	95.01	89.93
Sample4Geo[12]	100(%)	92.65	93.81	95.14	91.39
CAMP[40]	100(%)	94.46	95.38	96.15	92.72
DAC[41]	100(%)	94.67	95.50	96.43	93.79
CDIKTNet	100(%)	95.02	95.79	96.15	93.93
CDIKTNet	10(%)	88.02	89.84	93.87	86.48
CDIKTNet	2(%)	85.63	87.75	90.44	82.24
CDIKTNet	0(%)	83.30	85.73	87.73	76.53

Table 2. Comparisons between the proposed CDIKTNet and some state-of-the-art methods on the University-1652 datasets.

retrieved results, while AP represents the balance between precision and recall.

4.2. Implementation Details

During training and testing, all input images are resized to $3 \times 384 \times 384$. The cross-domain invariance sub-network is trained for 1 epoch, while the domain adaptation process runs for 30 epochs, with a batch size of 64. The DBSCAN [14] is used to generate pseudo-labels. For optimization, the AdamW optimizer is used for the cross-domain invariance sub-network with an initial learning rate of 0.001, followed by SGD optimization for the domain adaptation sub-network with a learning rate of 0.00025. Furthermore, in Eq.(7), λ_1 , λ_2 , and λ_3 are set to 0.6, 0.1, and 1, respectively. The CDTS is activated only when unpaired data is present. In the two benchmarks, each location has a single satellite image, which is replicated 50 times for clustering.

4.3. Comparison with State-of-the-art Methods

We conduct experiments with three settings, including fully supervised, few-shot initialization, and cross-domain initialization. Our CDIKTNet is compared with existing state-

of-the-art methods on two benchmarks including SUES-200 and University-1652. The results on SUES-200 and University-1652 and are reported in Table 1 and Table 2, respectively. Additionally, we evaluate the cross-domain generalization ability, with results presented in Table 3.

Fully Supervised: In the fully supervised setting, we utilize all paired data, as shown in Table 2 and Table 1. Compared with existing state-of-the-art methods, CDIKTNet achieves superior performance on both benchmarks. Specifically, on University-1652, it attains 95.02% R@1 and 95.79% AP in drone→satellite, while ranking second in satellite→drone but still achieving the highest AP. On SUES-200, across two elevate modes and four altitude levels, CDIKTNet consistently outperforms advanced methods such as DAC [41] and CAMP [40] and significantly surpasses Sample4Geo [12] in evaluation. Furthermore, as shown in the generalization evaluation as shown in Table 3, CDIKTNet exhibits superior generalization ability, which is critical for open-world applications. These results confirm its effectiveness in learning robust cross-view features.

Few-shot Initialization: To evaluate the effectiveness of CDIKTNet in leveraging unlabeled data for learning, we initialize CDIKTNet with only 2% and 10% of the paired data. The rest of the paired data in the dataset is transformed into unpaired data and further used to simulate the scenarios that are difficult to obtain the pairing relationships. Tables 2 and 1 show that even with only 2% of the paired data, our method effectively exploits cross-view information from unpaired data, achieving performance comparable to or even surpassing that of IFSs [48]. With 10%, CDIKTNet achieves further improvements, surpassing most fully supervised methods and achieving performance comparable to MCCG [31]. In particular, as shown in Table 3, CDIKTNet trained with 10% paired data achieves superior generalization, outperforming fully supervised methods. This highlights the importance of using unpaired data to uncover deeper cross-view representations.

Cross-domain Initialization: We propose a novel cross-domain validation setting. We initialize CDIKTNet with a

University-1652→SUES-200																	
Model	GT Ratio	Drone→Satellite								Satellite→Drone							
		150m		200m		250m		300m		150m		200m		300m		300m	
		R@1	AP	R@1	AP	R@1	AP	R@1	AP	R@1	AP	R@1	AP	R@1	AP	R@1	AP
MCCG[31]	100(%)	57.62	62.80	66.83	71.60	74.25	78.35	82.55	85.27	61.25	53.51	82.50	67.06	81.25	74.99	87.50	80.20
Sample4Geo[12]	100(%)	70.05	74.93	80.68	83.90	87.35	89.72	90.03	91.91	83.75	73.83	91.25	83.42	93.75	89.07	93.75	90.66
DAC[41]	100(%)	76.65	80.56	86.45	89.00	92.95	94.18	94.53	95.45	87.50	79.87	96.25	88.98	95.00	92.81	96.25	94.00
CAMP[40]	100(%)	78.90	82.38	86.83	89.28	91.95	93.63	95.68	96.65	87.50	78.98	95.00	87.05	95.00	91.05	96.25	93.44
CDIKTNet	100(%)	80.20	81.20	88.85	90.65	93.32	94.51	94.10	95.16	90.00	82.85	93.75	89.92	96.25	92.48	95.00	93.62
CDIKTNet	10(%)	81.35	84.28	89.15	91.16	94.18	95.29	96.68	97.32	91.25	81.10	97.50	90.44	98.75	93.87	98.75	95.05
CDIKTNet	2(%)	70.98	75.15	80.18	83.47	87.05	89.36	87.05	94.37	81.25	71.05	92.50	81.20	92.50	87.60	96.25	91.49

Table 3. Comparisons between the proposed CDIKTNet and existing state-of-the-art methods in cross-domain evaluation.

SUES-200																	
Model	GT Ratio	Drone→Satellite								Satellite→Drone							
		150m		200m		250m		300m		150m		200m		300m		300m	
		R@1	AP	R@1	AP	R@1	AP	R@1	AP	R@1	AP	R@1	AP	R@1	AP	R@1	AP
Sample4Geo[12]	2(%)	62.10	68.11	69.85	74.93	74.85	79.14	76.40	80.33	77.50	57.91	88.75	70.17	91.25	76.99	90.00	78.89
CAMP[40]	2(%)	54.73	61.70	62.30	68.39	65.83	71.42	68.40	73.58	68.75	49.25	82.50	60.49	87.50	68.79	91.25	74.43
DAC[41]	2(%)	55.83	62.16	68.50	73.25	73.38	77.34	74.70	78.64	70.00	51.09	85.00	61.59	90.00	70.53	91.25	74.63
CDIKTNet	2(%)	80.55	83.58	88.05	90.10	91.28	93.13	94.48	96.12	90.00	77.16	91.25	85.92	97.50	91.36	97.50	94.07
Sample4Geo	10(%)	75.43	79.21	84.20	86.70	87.18	89.40	89.63	91.61	91.25	76.89	92.50	82.76	96.25	86.60	96.25	89.23
CAMP	10(%)	76.27	80.39	83.83	86.89	89.66	91.62	90.85	92.71	92.50	77.50	96.25	86.63	97.50	91.45	97.50	93.29
DAC	10(%)	76.80	80.65	85.05	87.65	88.80	90.81	90.58	92.32	93.75	79.06	97.50	86.78	97.50	90.58	98.75	92.54
CDIKTNet	10(%)	83.60	86.24	90.53	92.14	94.33	95.32	97.13	97.60	91.25	83.24	95.00	89.52	97.50	93.59	97.50	95.80

Table 4. Comparisons between the proposed CDIKTNet and existing state-of-the-art methods on the SUES-200 when training data is only 2(%) and 10(%) paired data.

University-1652						
Model	GT Ratio	Drone→Satellite		Satellite→Drone		
		R@1	AP	R@1	AP	
Sample4Geo[12]	2(%)	62.41	66.85	84.45	60.52	
CAMP[40]	2(%)	62.53	67.01	83.31	59.26	
DAC[41]	2(%)	63.68	68.16	87.59	61.26	
CDIKTNet	2(%)	85.63	87.75	90.44	82.24	
CAMP[40]	10(%)	83.64	86.27	92.44	82.27	
Sample4Geo[12]	10(%)	84.51	86.94	93.01	83.53	
DAC[41]	10(%)	84.64	87.07	93.15	83.03	
CDIKTNet	10(%)	88.02	89.84	93.87	86.48	

Table 5. Comparisons between the proposed CDIKTNet and existing state-of-the-art methods on the University-1652 when training data is only 2(%) and 10(%) paired data.

small amount of paired data and train it using the remaining unpaired data. This trained model is then transferred to another benchmark for further training without requiring additional pairing relationships, with the supervision ratio considered 0% during the transfer phase. The reverse validation follows the same procedure. As shown in Table 2 and Table 1, after training in one domain, CDIKTNet can be directly transferred to another without re-paired data, achieving test performance comparable to fully supervised methods on both datasets. Notably, in the SUES-200 dataset, the proposed cross-domain training method demonstrates superior performance compared with the initialization utilizing 2% of paired data. This suggests that when the model exhibits strong adaptability to domain shifts, cross-domain initialization can, in certain scenarios, even surpass direct training with a limited amount of paired data.

Furthermore, to better highlight the distinctions between our approach and existing methods, we present a comparative analysis under the initialization with 2% and 10% of paired data, as shown in Table 4 and Table 5. Existing supervised methods strictly rely on paired data as positive samples for training and cannot utilize unpaired data. Therefore, we evaluate these advanced methods using only 2% of paired data. The results show that under this extreme condition, existing methods fail to exploit cross-view feature information, whereas CDIKTNet effectively leverages such information, significantly outperforming these methods, and reducing the reliance on costly paired annotations.

4.4. Ablation Studies

In this section, we meticulously carry out ablation experiments to validate the effectiveness of each component in CDIKTNet. The results are reported in Table 6.

Effectiveness of Cross-Domain Invariance Sub-network: The SIFL and the SIEL significantly improve the UVGL accuracy across different settings. Notably, their combined use leads to even greater performance gains, validating the core principle of the CDIS. Structural features capture geometric invariance across views, while spatial features enhance spatial consistency by incorporating scale awareness. These two types of features complement each other, forming a dynamic joint representation and establishing a robust feature space.

Effectiveness of Cross-Domain Transfer Subnetwork: The CDTS constructs a feature embedding space leverag-

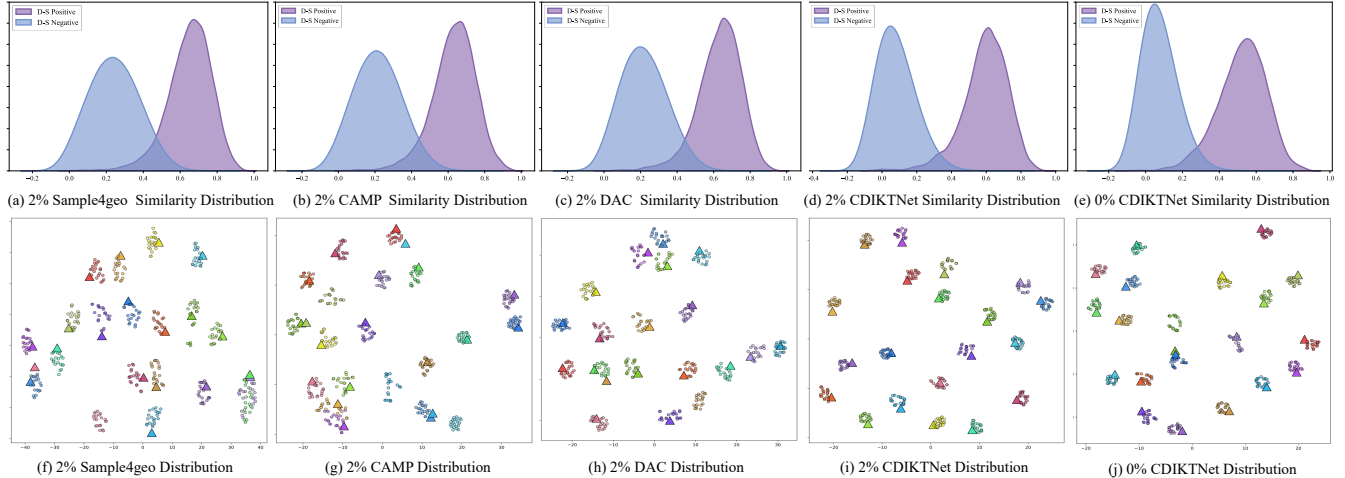


Figure 3. (a-e) show the similarity distribution visualization. (f-j) show the distribution of feature embeddings in the 2D feature space, where circles and triangles in different colors denote drone and satellite view. A total of 20 localizations are selected from the test set.

University-1652							
	Setting			Drone \rightarrow Satellite		Satellite \rightarrow Drone	
	SIFL	SIEL	CDTS	R@1	AP	R@1	AP
2%	✓			58.19	62.69	82.45	56.95
		✓		59.00	63.55	81.16	55.03
	✓	✓		59.73	64.16	80.03	57.35
	✓	✓	✓	63.93	68.19	83.45	61.35
			85.63	87.75	90.44	82.24	
100%				92.80	94.00	95.01	91.83
	✓			94.02	94.96	95.72	93.16
		✓		93.26	94.36	95.58	92.15
	✓	✓		95.02	95.79	96.15	93.93

Table 6. The influence of each component on the performance of the proposed CDIKTNet.

ing invariance knowledge, demonstrating robust optimization capabilities even under extreme scarcity of paired data. Moreover, as the proportion of paired data increases and our method achieves strong performance using the available pairs, the CDTS continues to enhance overall network performance by further exploiting the latent cross-view characteristics of unpaired data.

4.5. Visualization

Feature distribution. We perform feature space visualization (t-SNE [37]) and similarity distribution analysis to compare CDIKTNet with existing state-of-the-art methods, where 2% represents the supervision ratio, as shown in Fig. 3. Regardless of whether CDIKTNet is initialized with 2% of paired data or trained using a 0% supervision transfer strategy, it significantly enhances the separation of cross-view positive and negative distributions compared to existing state-of-the-art methods. This demonstrates the effectiveness of our method in addressing cross-view discrepan-

cies and using unpaired data for learning.

5. Conclusion

This paper addresses a critical and highly challenging problem for the UAV-View Geo-Localization (UVGL) task with minimal or even no paired data to reduce dependence on expensive cross-view annotations. To this end, we propose a novel cross-domain invariance knowledge transfer network (CDIKTNet), which captures the spatial and structural invariances of cross-view features while constructing a robust invariant knowledge representation space. Meanwhile, it utilizes this embedding space as an optimization anchor for self-supervised training, effectively learning latent cross-view information from unpaired data. It significantly alleviates the reliance on paired data. More importantly, CDIKTNet can generalize to new environments without requiring any prior pairing relationships. Extensive experiments show that, under fully supervised setting, CDIKTNet outperforms existing state-of-the-art methods. Furthermore, when initialized with a small amount of paired data and then trained via self-supervised learning or transferring for other scenarios to further self-supervised learning, CDIKTNet even surpasses some fully supervised counterparts, propelling UVGL toward real-world deployment.

Acknowledgments

This work was supported in part by the Key Research and Development Program of Shaanxi, PR China (No. 2023-YGBY-235), the National Natural Science Foundation of China (No. 61976172 and No. 12002254), Major Scientific and Technological Innovation Project of Xianyang, PR China (No. L2023-ZDKJ-JSGG-GY-018).

References

- [1] Woo-Jin Ahn, So-Yeon Park, Dong-Sung Pae, Hyun-Duck Choi, and Myo-Taeg Lim. Bridging viewpoints in cross-view geo-localization with siamese vision transformer. *IEEE Transactions on Geoscience and Remote Sensing*, 62:1–12, 2024. 2
- [2] Alberto Baldrati, Marco Bertini, Tiberio Uricchio, and Alberto Del Bimbo. Effective conditioned and composed image retrieval combining clip-based features. In *Proceedings of the IEEE/CVF Conference on Computer Vision and Pattern Recognition (CVPR)*, pages 21466–21474, 2022. 2
- [3] Sudong Cai, Yulan Guo, Salman Khan, Jiwei Hu, and Gongjian Wen. Ground-to-aerial image geo-localization with a hard exemplar reweighting triplet loss. In *Proceedings of the IEEE/CVF International Conference on Computer Vision (ICCV)*, pages 8391–8400, 2019. 1
- [4] Mathilde Caron, Piotr Bojanowski, Armand Joulin, and Matthijs Douze. Deep clustering for unsupervised learning of visual features. In *Proceedings of the European Conference on Computer Vision (ECCV)*, pages 132–149, 2018. 3
- [5] Mathilde Caron, Ishan Misra, Julien Mairal, Priya Goyal, Piotr Bojanowski, and Armand Joulin. Unsupervised learning of visual features by contrasting cluster assignments. *Advances in neural information processing systems*, 33:9912–9924, 2020. 3
- [6] Hao Chen, Benoit Lagadec, and François Bremond. Ice: Inter-instance contrastive encoding for unsupervised person re-identification. In *Proceedings of the IEEE/CVF International Conference on Computer Vision (ICCV)*, pages 14960–14969, 2021. 3
- [7] Quan Chen, Tingyu Wang, Zihao Yang, Haoran Li, Rongfeng Lu, Yaoqi Sun, Bolun Zheng, and Chenggang Yan. SDPL: Shifting-dense partition learning for UAV-view geo-localization. *IEEE Transactions on Circuits and Systems for Video Technology*, 34(11):11810–11824, 2024. 2
- [8] Yanbei Chen and Loris Bazzani. Learning joint visual semantic matching embeddings for language-guided retrieval. In *Proceedings of the European Conference on Computer Vision (ECCV)*, pages 136–152, 2020. 2
- [9] Zhongwei Chen, Zhao-Xu Yang, and Hai-Jun Rong. Multi-level embedding and alignment network with consistency and invariance learning for cross-view geo-localization. *arXiv preprint arXiv:2412.14819*, 2024. 1
- [10] Ming Dai, Enhui Zheng, Zhenhua Feng, Lei Qi, Jiedong Zhuang, and Wankou Yang. Vision-based uav self-positioning in low-altitude urban environments. *IEEE Transactions on Image Processing*, 33:493–508, 2024. 1
- [11] Zuozhuo Dai, Guangyuan Wang, Weihao Yuan, Siyu Zhu, and Ping Tan. Cluster contrast for unsupervised person re-identification. In *Proceedings of the Asian conference on computer vision*, pages 1142–1160, 2022. 3
- [12] Fabian Deuser, Konrad Habel, and Norbert Oswald. Sample4Geo: Hard negative sampling for cross-view geo-localisation. In *Proceedings of the IEEE/CVF International Conference on Computer Vision (ICCV)*, pages 16847–16856, 2023. 1, 6, 7
- [13] Haolin Du, Jingfei He, and Yuanqing Zhao. CCR: A counterfactual causal reasoning-based method for cross-view geo-localization. *IEEE Transactions on Circuits and Systems for Video Technology*, 34(11):11630–11643, 2024. 2
- [14] Martin Ester, Hans-Peter Kriegel, Jörg Sander, Xiaowei Xu, et al. A density-based algorithm for discovering clusters in large spatial databases with noise. In *kdd*, pages 226–231, 1996. 3, 6
- [15] Xingye Fang, Yang Yang, and Ying Fu. Visible-infrared person re-identification via semantic alignment and affinity inference. In *Proceedings of the IEEE/CVF International Conference on Computer Vision (ICCV)*, pages 11270–11279, 2023. 2
- [16] Fawei Ge, Yunzhou Zhang, Yixiu Liu, Guiyuan Wang, Sonya Coleman, Dermot Kerr, and Li Wang. Multibranch joint representation learning based on information fusion strategy for cross-view geo-localization. *IEEE Transactions on Geoscience and Remote Sensing*, 62:1–16, 2024. 2, 6
- [17] Ian Goodfellow, Jean Pouget-Abadie, Mehdi Mirza, Bing Xu, David Warde-Farley, Sherjil Ozair, Aaron Courville, and Yoshua Bengio. Generative adversarial nets. *Advances in neural information processing systems*, 27:2672–2680, 2014. 2
- [18] Kaiming He, Haoqi Fan, Yuxin Wu, Saining Xie, and Ross Girshick. Momentum contrast for unsupervised visual representation learning. In *Proceedings of the IEEE/CVF Conference on Computer Vision and Pattern Recognition (CVPR)*, pages 9729–9738, 2020. 3
- [19] Wenmiao Hu, Yichen Zhang, Yuxuan Liang, Yifang Yin, Andrei Georgescu, An Tran, Hannes Kruppa, See-Kiong Ng, and Roger Zimmermann. Beyond geo-localization: Fine-grained orientation of street-view images by cross-view matching with satellite imagery. In *Proceedings of the 30th ACM International Conference on Multimedia*, page 6155–6164, 2022. 2
- [20] Yuxiang Ji, Boyong He, Zhuoyue Tan, and Liaoni Wu. Game4loc: A uav geo-localization benchmark from game data. *arXiv preprint arXiv:2409.16925*, 2024. 2
- [21] Bowen Li, Ziyuan Huang, Junjie Ye, Yiming Li, Sebastian Scherer, Hang Zhao, and Changhong Fu. Pvt++: A simple end-to-end latency-aware visual tracking framework. In *Proceedings of the IEEE/CVF International Conference on Computer Vision (ICCV)*, pages 10006–10016, 2023. 1
- [22] Guopeng Li, Ming Qian, and Gui-Song Xia. Unleashing unlabeled data: A paradigm for cross-view geo-localization. In *Proceedings of the IEEE/CVF Conference on Computer Vision and Pattern Recognition (CVPR)*, pages 16719–16729, 2024. 1
- [23] Liu Liu and Hongdong Li. Lending orientation to neural networks for cross-view geo-localization. In *Proceedings of the IEEE/CVF Conference on Computer Vision and Pattern Recognition (CVPR)*, page 5624–5633, 2019. 2
- [24] Shuai Liu, Xin Li, Huchuan Lu, and You He. Multi-object tracking meets moving uav. In *Proceedings of the IEEE/CVF Conference on Computer Vision and Pattern Recognition (CVPR)*, pages 8876–8885, 2022. 1
- [25] Zhuang Liu, Hanzi Mao, Chao-Yuan Wu, Christoph Feichtenhofer, Trevor Darrell, and Saining Xie. A convnet for the

- 2020s. In *Proceedings of IEEE/CVF Conference on Computer Vision and Pattern Recognition (CVPR)*, pages 11976–11986, 2022. 3
- [26] Hongxiang Lv, Hai Zhu, Runzhe Zhu, Fei Wu, Chunyuan Wang, Meiyu Cai, and Kaiyu Zhang. Direction-guided multi-scale feature fusion network for geo-localization. *IEEE Transactions on Geoscience and Remote Sensing*, 62: 1–13, 2024. 2
- [27] James MacQueen et al. Some methods for classification and analysis of multivariate observations. In *Proceedings of the fifth Berkeley symposium on mathematical statistics and probability*, pages 281–297, 1967. 3
- [28] Aaron van den Oord, Yazhe Li, and Oriol Vinyals. Representation learning with contrastive predictive coding. *arXiv preprint arXiv:1807.03748*, 2018. 5
- [29] Ming Qian, Jincheng Xiong, Gui-Song Xia, and Nan Xue. Sat2density: Faithful density learning from satellite-ground image pairs. In *Proceedings of the IEEE/CVF International Conference on Computer Vision (ICCV)*, pages 3683–3692, 2023. 1
- [30] Krishna Regmi and Mubarak Shah. Bridging the domain gap for ground-to-aerial image matching. In *Proceedings of the IEEE/CVF International Conference on Computer Vision (ICCV)*, pages 470–479, 2019. 2
- [31] Tianrui Shen, Yingmei Wei, Lai Kang, Shanshan Wan, and Yee-Hong Yang. MCCG: A convnext-based multiple-classifier method for cross-view geo-localization. *IEEE Transactions on Circuits and Systems for Video Technology*, 34(3):1456–1468, 2023. 2, 4, 5, 6, 7
- [32] Yujiao Shi, Liu Liu, Xin Yu, and Hongdong Li. Spatial-aware feature aggregation for image based cross-view geo-localization. *Advances in Neural Information Processing Systems*, 32:10090–10100, 2019. 2
- [33] Yujiao Shi, Xin Yu, Dylan Campbell, and Hongdong Li. Where am i looking at? joint location and orientation estimation by cross-view matching. In *Proceedings of the IEEE/CVF Conference on Computer Vision and Pattern Recognition (CVPR)*, pages 4064–4072, 2020. 1
- [34] Yujiao Shi, Xin Yu, Liu Liu, Tong Zhang, and Hongdong Li. Optimal feature transport for cross-view image geo-localization. In *Proceedings of the AAAI Conference on Artificial Intelligence (AAAI)*, pages 11990–11997, 2020. 2
- [35] Xiaoyang Tian, Jie Shao, Deqiang Ouyang, and Heng Tao Shen. UAV-satellite view synthesis for cross-view geo-localization. *IEEE Transactions on Circuits and Systems for Video Technology*, 32(7):4804–4815, 2021. 2
- [36] Aysim Toker, Qunjie Zhou, Maxim Maximov, and Laura Leal-Taixe. Coming down to earth: Satellite-to-street view synthesis for geo-localization. In *Proceedings of the IEEE/CVF Conference on Computer Vision and Pattern Recognition (CVPR)*, pages 6488–6497, 2021. 2
- [37] Laurens Van der Maaten and Geoffrey Hinton. Visualizing data using t-SNE. *Journal of machine learning research*, 9(11):2579–2605, 2008. 8
- [38] Tingyu Wang, Zhedong Zheng, Chenggang Yan, Jiyong Zhang, Yaoqi Sun, Bolun Zheng, and Yi Yang. Each part matters: Local patterns facilitate cross-view geo-localization. *IEEE Transactions on Circuits and Systems for Video Technology*, 32(2):867–879, 2021. 6
- [39] Tingyu Wang, Zhedong Zheng, Yaoqi Sun, Chenggang Yan, Yi Yang, and Tat-Seng Chua. Multiple-environment self-adaptive network for aerial-view geo-localization. *Pattern Recognition*, 152:110363, 2024. 6
- [40] Qiong Wu, Yi Wan, Zhi Zheng, Yongjun Zhang, Guangshuai Wang, and Zhenyang Zhao. CAMP: Across-view geo-localization method using contrastive attributes mining and position-aware partitioning. *IEEE Transactions on Geoscience and Remote Sensing*, 62:1–14, 2024. 1, 6, 7
- [41] Panwang Xia, Yi Wan, Zhi Zheng, Yongjun Zhang, and Jiwei Deng. Enhancing cross-view geo-localization with domain alignment and scene consistency. *IEEE Transactions on Circuits and Systems for Video Technology*, pages 1–12, 2024. 2, 5, 6, 7
- [42] Peng Xu and Xiatian Zhu. Deepchange: A long-term person re-identification benchmark with clothes change. In *Proceedings of the IEEE/CVF International Conference on Computer Vision (ICCV)*, pages 11196–11205, 2023. 2
- [43] Shiyu Xuan and Shiliang Zhang. Intra-inter camera similarity for unsupervised person re-identification. In *Proceedings of the IEEE/CVF Conference on Computer Vision and Pattern Recognition (CVPR)*, pages 11926–11935, 2021. 3
- [44] Bin Yang, Mang Ye, Jun Chen, and Zesen Wu. Augmented dual-contrastive aggregation learning for unsupervised visible-infrared person re-identification. In *Proceedings of the 30th ACM International Conference on Multimedia*, pages 2843–2851, 2022. 3
- [45] Bin Yang, Jun Chen, and Mang Ye. Shallow-deep collaborative learning for unsupervised visible-infrared person re-identification. In *Proceedings of the IEEE/CVF Conference on Computer Vision and Pattern Recognition (CVPR)*, pages 16870–16879, 2024. 3
- [46] Xiaohan Zhang, Xingyu Li, Waqas Sultani, Yi Zhou, and Safwan Wshah. Cross-view geo-localization via learning disentangled geometric layout correspondence. In *Proceedings of the AAAI Conference on Artificial Intelligence (AAAI)*, pages 3480–3488, 2023. 1, 2
- [47] Yukang Zhang and Hanzi Wang. Diverse embedding expansion network and low-light cross-modality benchmark for visible-infrared person re-identification. In *Proceedings of the IEEE/CVF Conference on Computer Vision and Pattern Recognition (CVPR)*, pages 2153–2162, 2023. 2
- [48] Hu Zhao, Keyan Ren, Tianyi Yue, Chun Zhang, and Shuai Yuan. TransFG: A cross-view geo-localization of satellite and UAVs imagery pipeline using transformer-based feature aggregation and gradient guidance. *IEEE Transactions on Geoscience and Remote Sensing*, 62:1–12, 2024. 6
- [49] Zhedong Zheng, Yunchao Wei, and Yi Yang. University-1652: A multi-view multi-source benchmark for drone-based geo-localization. In *Proceedings of the 28th ACM International Conference on Multimedia*, page 1395–1403, 2020. 5
- [50] Runzhe Zhu, Ling Yin, Mingze Yang, Fei Wu, Yuncheng Yang, and Wenbo Hu. SUES-200: A multi-height multi-scene cross-view image benchmark across drone and satel-

lite. *IEEE Transactions on Circuits and Systems for Video Technology*, 33(9):4825–4839, 2023. [5](#), [6](#)